



TITLE:

# Momentum Equations of the Boundary Layer and their Application to the Turbulent Boundary Layer

AUTHOR(S):

HUDIMOTO, Busuke

---

CITATION:

HUDIMOTO, Busuke. Momentum Equations of the Boundary Layer and their Application to the Turbulent Boundary Layer. *Memoirs of the Faculty of Engineering, Kyoto University* 1951, 13(4): 162-173

ISSUE DATE:

1951-11-10

URL:

<http://hdl.handle.net/2433/280240>

RIGHT:

# Momentum Equations of the Boundary Layer and their Application to the Turbulent Boundary Layer

By

Busuke HUDIMOTO

Department of Applied Physics

(Received June, 1951)

The momentum equation of the boundary layer was first found by v. Kármán (reference 1) and was used in the approximate calculation of the boundary layer problems. Kármán-Pohlhausen's solution of laminar boundary layer (reference 2) is a well-known one. But as the velocity distribution is expressed by one parameter, this method loses accuracy at, and in the neighbourhood of, the separation point. To improve the method, it is necessary add another parameter to the expression of the velocity distribution.

The theory of turbulence has already been well developed and much of it is known but little is known about the turbulent flow with pressure rise and fall. So it seems difficult to develop a theoretical method of calculating turbulent boundary layer; yet if a simple and practical method can be obtained, it will be useful in the field of hydraulic engineering. Hitherto there have been two well-known methods, one being that of Buri (reference 3) and the other that of Gruschwitz (reference 4). Buri's method is easy to calculate but does not give any reliable result about the separation of boundary layer. To calculate both the thickness and the velocity distribution of the boundary layer, at least two equations are needed, and Gruschwitz uses momentum equation and an empirical relation which is obtained from his experimental result.

To improve the solution of the laminar boundary layer problem and to solve the turbulent boundary layer problem, the author has derived an equation of momentum applying the law of moment of momentum. And a method of calculating turbulent boundary layer has been developed by using the above-mentioned momentum equation.

## 1. Equations of Momentum

Take rectangular coordinate axes  $x$  and  $y$ ,  $x$ -axis being along the surface of body, and let  $u$  be the  $x$ -component,  $v$  the  $y$ -component of velocity,  $u_0$  the velocity

outside the boundary layer,  $\tau$  the shearing stress,  $p$  the static pressure, and  $\rho$  the density of fluid, then the equations of motion and continuity in the case of steady flow are as follows:

$$u \frac{\partial u}{\partial x} + v \frac{\partial u}{\partial y} = -\frac{1}{\rho} \cdot \frac{dp}{dx} + \frac{1}{\rho} \cdot \frac{\partial \tau}{\partial y}, \quad (1)$$

$$\frac{\partial u}{\partial x} + \frac{\partial v}{\partial y} = 0. \quad (2)$$

Integrating eq. (1) from  $y=0$  the surface of body to  $y=\delta$ ,  $\delta$  being the boundary layer thickness,

$$\frac{d}{dx} \int_0^\delta u^2 dy - u_0 \frac{d}{dx} \int_0^\delta u dy = \delta u_0 \frac{du_0}{dx} - \frac{\tau_0}{\rho}, \quad (3)$$

where  $\tau_0$  is the shearing stress at  $y=0$ .

Eq. (3) is the Kármán's momentum equation (reference 3) and this can also be obtained by applying law of momentum.

Multiply  $y$  on both sides of eq. (1) and integrate from  $y=0$  to  $y=\delta$ , then

$$\frac{d}{dx} \int_0^\delta u^2 y dy - u_0 \delta \frac{d}{dx} \int_0^\delta u dy - \int_0^\delta u v dy = \frac{\delta^2 u_0}{2} \cdot \frac{du_0}{dx} - \frac{1}{\rho} \int_0^\delta \tau dy. \quad (4)$$

This equation can also be obtained by applying law of moment of momentum. Take a small portion  $OABC$  of the boundary layer as shown in Fig. 1 and consider moment around  $O$ , then

$$\frac{d}{dx} \int_0^\delta \rho u^2 y dy \cdot dx - u_0 \delta \frac{d}{dx} \int_0^\delta \rho u dy \cdot dx - \int_0^\delta \rho u v dy \cdot dx$$

is the excess of moment of momentum around  $O$  which is carried away by the outgoing fluid from the region  $OABC$ . While

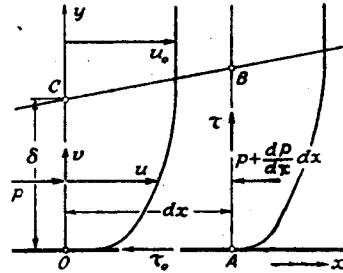


Fig. 1.

$$-\frac{\delta^2}{2} \cdot \frac{dp}{dx} dx - \int_0^\delta \tau dy \cdot dx = \frac{\delta^2 u_0}{2} \cdot \frac{du_0}{dx} dx - \int_0^\delta \tau dy \cdot dx$$

is the moment of force acting on the fluid in  $OABC$ . Equating these two quantities eq. (4) is obtained.

Eqs. (3) and (4) hold in both cases of laminar and turbulent flows and in the present calculation these two equations are applied.

## 2. Velocity Distribution of Turbulent Flow

To apply eqs. (3) and (4), velocity distribution in the boundary layer is to be properly assumed as in the case of Kármán-Pohlhausen's method with laminar flow.

Assuming velocity distribution changes gradually in the direction of  $x$ , velocity distribution in the boundary layer is expressed as follows:

$$\frac{u}{u_0} = \kappa F(\eta) + (1 - \kappa)G(\eta), \tag{5}$$

where  $\kappa$  is a dimensionless parameter,  $F(\eta)$  and  $G(\eta)$  are functions of  $\eta = \frac{y}{\delta}$ .

As  $F(\eta)$ , the velocity distribution on a flat plate placed along the direction of uniform flow is taken. The shearing stress distribution in the boundary layer is assumed as follows:

$$\frac{\tau}{\tau_0} = 1 - 0.225\eta - 2.55\eta^2 + 1.775\eta^3. \tag{6}$$

The second term on the right hand side is determined after some theoretical consideration assuming  $\frac{u_0\delta}{\nu}$  is not so large,  $\nu$  being the kinematic coefficient of viscosity, and this distribution agrees with experimental result (reference 5). And mixing length  $l_1$  in the boundary layer is assumed from the experimental result of Schultz-Grunow as shown in Fig. 2 and Table 1. Then,

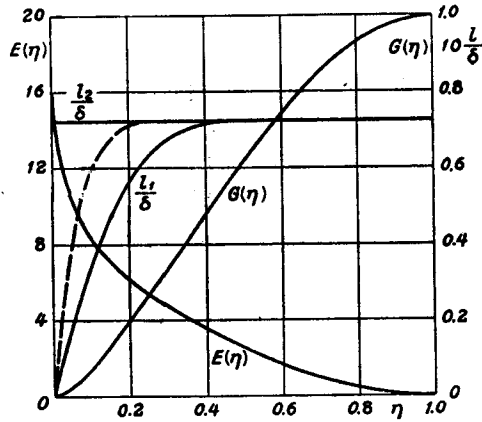


Fig. 2.

Table 1.

$\eta$	$\frac{l_1}{\delta}$	$E(\eta)$	$-\frac{dE}{d\eta}$
0	0	—	—
0.05	0.01967	10.2345	50.395
0.1	0.03513	8.2795	27.800
0.15	0.04737	7.1120	20.192
0.2	0.05660	6.1959	16.453
0.3	0.06765	4.7579	12.809
0.4	0.07168	3.5774	10.946
0.5	0.07220	2.5553	9.514
0.6	0.07220	1.6799	7.961
0.7	0.07220	0.9693	6.222
0.8	0.07220	0.4413	4.309
0.9	0.07220	0.1129	2.232
1.0	0.07220	0	0

$$\frac{\tau}{\rho u_0^2} = \left(\frac{l_1}{\delta}\right)^2 \left(\frac{dF}{d\eta}\right)^2.$$

Integrating above equation numerically and putting  $\frac{\tau_0}{\rho u_0^2} = \zeta_0$  and  $\sigma = \sqrt{\zeta_0}$ ,

$$F(\eta) = 1 - \sigma E(\eta). \tag{7}$$

$\sigma$  is equal to the ratio between friction velocity and  $u_0$ .  $E(\eta)$  is a function of  $\eta$  and is shown in Fig. 2 and Table 1 with  $\frac{dE}{d\eta}$ . The calculated result exactly coin-

cides with the measured velocity distribution of Schultz-Grunow (reference 5).

As  $G(\eta)$ , the extreme case of the state of separation of boundary layer is taken. When the boundary layer is in the state of separation, the shearing stress distribution may be assumed as follows:

$$\tau = \text{const. } \eta(1-\eta)^2. \quad (8)$$

Assuming the mixing length  $l_2$  is constant throughout the boundary layer,

$$\left(\frac{l_2}{\delta}\right)^2 \left(\frac{dG}{d\eta}\right)^2 = \text{const. } \eta(1-\eta)^2.$$

Inregrating the above equation and by the conditions  $G(\eta)=0$  at  $\eta=0$ , and  $G(\eta)=1$  at  $\eta=1$ ,

$$G(\eta) = \eta^{\frac{3}{2}}(2.5-1.5\eta). \quad (9)$$

Values of  $G(\eta)$  are given in Fig. 2 and Table 2.

Combining  $F(\eta)$  and  $G(\eta)$  as eq. (5), the assumed velocity distribution when  $\sigma=0.04$  becomes as shown in Fig. 3.

Table 2.

$\eta$	$F'(\eta)$	$\frac{dF'}{d\eta}$	$G(\eta)$	$\frac{dG}{d\eta}$
0	0.388	—	0	0
0.05	0.639	1.600	0.0271	0.7965
0.1	0.702	0.9163	0.0743	1.0672
0.15	0.744	0.7248	0.1322	1.2345
0.2	0.777	0.6136	0.1968	1.3416
0.3	0.833	0.4778	0.3368	1.4378
0.4	0.876	0.3918	0.4807	1.4231
0.5	0.912	0.3214	0.6187	1.3258
0.6	0.942	0.2628	0.7436	1.1619
0.7	0.966	0.2002	0.8496	0.9413
0.8	0.983	0.1432	0.9302	0.6708
0.9	0.995	0.0852	0.9819	0.3558
1.0	1.000	0	1.0000	0

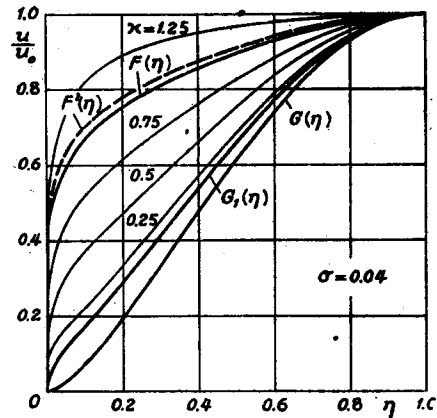


Fig. 3.

In obtaining  $G(\eta)$ , it is assumed that the mixing length is constant but this is too much idealized. Assuming the same shearing stress distribution and taking  $\frac{l}{\delta}$  as shown in Fig. 2 by broken line which is estimated from Nikuradse's experiment (reference 6), the velocity distribution in the state of separation becomes as shown in Fig. 3 marked by  $G_1(\eta)$ .

There is another experimental result on the flow along the flat plate obtained by Nikuradse (reference 7) besides that of Schultz-Grunow. Nikuradse's velocity

distribution is shown in Fig. 3 by broken line and marked by  $F'(\eta)$ . If  $F'(\eta)$  is applied,

$$\frac{u}{u_0} = \kappa F'(\eta) + (1-\kappa)G(\eta). \tag{10}$$

Table 2 shows numerical values of  $F'(\eta)$  and  $\frac{dF'}{d\eta}$  with  $G(\eta)$  and  $\frac{dG}{d\eta}$ .

### 3. Several Quantities of Velocity Distribution

Let  $\frac{u}{u_0} = f(\eta)$  and

$$\int_0^1 f d\eta = k_1, \quad \int_0^1 f^2 d\eta = k_2, \quad \int_0^1 f^2 \eta d\eta = k_3, \\ \int_0^1 f \int_0^\eta f d\eta d\eta = k_4, \quad \int_0^1 f \int_0^\eta \frac{\partial f}{\partial \eta} \eta d\eta d\eta = k_5, \quad \int_0^1 f \int_0^\eta \frac{\partial f}{\partial \kappa} d\eta d\eta = k_6,$$

then the displacement thickness  $\delta^*$  and momentum thickness  $\theta$  of the boundary layer are

$$\delta^* = (1-k_1)\delta, \quad \theta = (k_1-k_2)\delta, \\ \text{and} \quad H = \frac{\delta^*}{\theta} = \frac{1-k_1}{k_1-k_2}. \tag{11}$$

From eq. (2)

$$v = -\int_0^y \frac{\partial u}{\partial x} dy,$$

and

$$\frac{\partial u}{\partial x} = f \frac{du_0}{dx} - u_0 \frac{\eta}{\delta} \cdot \frac{\partial f}{\partial \eta} \cdot \frac{d\delta}{dx} + u_0 \frac{\partial f}{\partial \kappa} \cdot \frac{d\kappa}{dx};$$

hence

$$\int_0^\delta uv dy = -u_0 \delta^2 \frac{du_0}{dx} k_4 + u_0^2 \delta \frac{d\delta}{dx} k_5 - u_0^2 \delta^2 \frac{d\kappa}{dx} k_6. \tag{12}$$

The shearing stress  $\tau$  is given by

$$\tau = \rho u_0^2 \left(\frac{l}{\delta}\right)^2 \left(\frac{\partial f}{\partial \eta}\right)^2,$$

but in the calculation of  $F(\eta)$  and  $G(\eta)$ , different values of the mixing length  $l$  in the neighbourhood of  $\eta=0$  are taken, so in calculating  $\tau$  the following relation is applied:

$$\frac{\tau}{\rho u_0^2} = \left(\kappa \frac{l_1}{\delta} \cdot \frac{dF}{d\eta} + (1-\kappa) \frac{l_2}{\delta} \cdot \frac{dG}{d\eta}\right)^2, \tag{13}$$

where  $l_2=0.0722\delta$ , and  $l_1$  is the mixing length used in the calculation of  $F(\eta)$ .

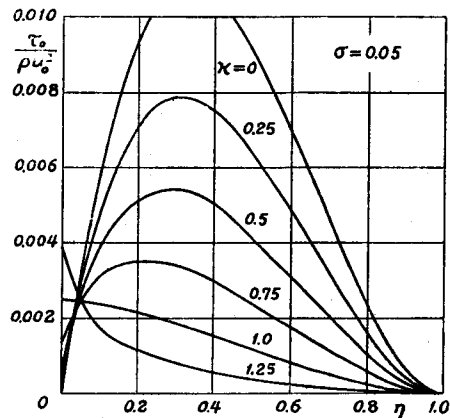


Fig. 4.

The shearing stress distribution when  $\sigma=0.05$  is shown in Fig. 4. The assumption of eq. (13) is crude and quite arbitrary and has no theoretical foundation, but since the knowledge about mixing length is scarce, this equation is applied in the present calculation.

Calculated values of  $k_1, k_2$ , etc. are as follow :

$$\begin{aligned} k_1 &= 0.5714 + 0.4286\kappa - 3.508\sigma\kappa, \\ k_2 &= 0.4375 + 0.2679\kappa - 1.875\sigma\kappa + 0.2946\kappa^2 - 5.141\sigma\kappa^2 + 23.9\sigma^2\kappa^2, \\ k_3 &= 0.3214 + 0.1190\kappa - 0.8036\sigma\kappa + 0.0595\kappa^2 - 0.884\sigma\kappa^2 + 3.32\sigma^2\kappa^2, \\ k_4 &= 0.1631 + 0.2452\kappa - 2.005\sigma\kappa + 0.0917\kappa^2 - 1.500\sigma\kappa^2 + 6.10\sigma^2\kappa^2, \\ k_5 &= 0.1582 - 0.1256\kappa + 1.197\sigma\kappa - 0.0323\kappa^2 + 0.613\sigma\kappa^2 - 2.76\sigma^2\kappa^2, \\ k_6 &= 0.2178 - 1.821\sigma + 0.0917\kappa - 1.500\sigma\kappa + 6.10\sigma^2\kappa, \\ k_7 &= \int_0^1 \frac{\tau}{\rho u_0^2} d\eta \\ &= 0.006109 - 0.012218\kappa + 0.10205\sigma\kappa + 0.006109\kappa^2 - 0.10205\sigma\kappa^2 + 0.484\sigma^2\kappa^2. \end{aligned}$$

Fig. 5, Tables 3, 4 and 5 show the value of  $\frac{\theta}{\delta}$  and  $H = \frac{\delta^*}{\theta}$ .

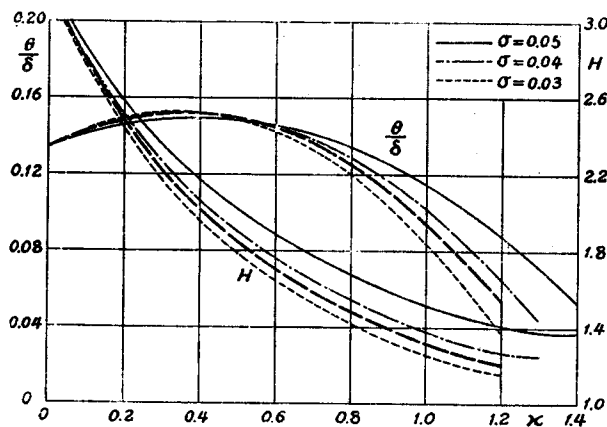


Fig. 5.

In the case of velocity distribution of eq. (10),

$$\begin{aligned} k_1 &= 0.5714 + 0.3041\kappa, \\ k_2 &= 0.4375 + 0.2022\kappa + 0.1413\kappa^2, \\ k_3 &= 0.3214 + 0.0908\kappa + 0.0323\kappa^2, \\ k_4 &= 0.1633 + 0.1737\kappa + 0.0464\kappa^2, \\ k_5 &= 0.1582 - 0.0844\kappa - 0.0142\kappa^2, \\ k_6 &= 0.1530 + 0.0464\kappa, \\ k_7 &= \int_0^1 \frac{\tau}{\rho u_0^2} d\eta \\ &= 0.00542 - 0.00625\kappa + 0.001963\kappa^2. \end{aligned}$$

Table 3.  $\sigma=0.03$ .

$\kappa$	$\frac{0}{\delta}$	$H$	$f_1(H)$	$f_2(H)$
0.1	0.1435	2.762	221.6	0.9743
0.2	0.1498	2.429	39.63	0.1663
0.3	0.1529	2.169	17.42	0.06705
0.4	0.1527	1.959	9.534	0.03234
0.5	0.1493	1.788	5.770	0.01650
0.6	0.1427	1.644	3.688	0.00841
0.7	0.1328	1.523	2.426	0.00407
0.8	0.1197	1.420	1.612	0.00174
0.9	0.1033	1.331	1.061	0.000537
1.0	0.0837	1.257	0.6715	-0.000017
1.1	0.0609	1.197	0.3805	-0.000188

Table 4.  $\sigma=0.04$ .

$\kappa$	$\frac{0}{\delta}$	$H$	$f_1(H)$	$f_2(H)$
0.1	0.1422	2.811	264.1	1.148
0.2	0.1479	2.508	48.73	0.2056
0.3	0.1511	2.264	22.01	0.08619
0.4	0.1517	2.065	12.36	0.04334
0.5	0.1498	1.899	7.685	0.02314
0.6	0.1454	1.759	5.054	0.01236
0.7	0.1384	1.639	3.436	0.00636
0.8	0.1288	1.537	2.375	0.00289
0.9	0.1167	1.449	1.647	0.000944
1.0	0.1021	1.375	1.125	-0.000078
1.1	0.0849	1.313	0.7323	-0.000507
1.2	0.0652	1.268	0.4040	-0.000512

Table 5.  $\sigma=0.05$ .

$\kappa$	$\frac{0}{\delta}$	$H$	$f_1(H)$	$f_2(H)$
0.1	0.1409	2.863	272.9	1.196
0.2	0.1459	2.591	58.31	0.2464
0.3	0.1489	2.368	27.50	0.1087
0.4	0.1500	2.182	15.95	0.05706
0.5	0.1491	2.025	10.20	0.03173
0.6	0.1463	1.891	6.896	0.01771
0.7	0.1416	1.775	4.825	0.00945
0.8	0.1349	1.676	3.443	0.00462
0.9	0.1262	1.590	2.477	0.00146
1.0	0.1157	1.517	1.773	-0.000258
1.1	0.1031	1.455	1.237	-0.00111
1.2	0.0886	1.407	0.800	-0.00132

Table 6.

$\kappa$	$\frac{0}{\delta}$	$H$	$f_1(H)$	$f_2(H)$
0.10	0.1427	2.790	210.8	0.6100
0.15	0.1460	2.623	77.73	0.2206
0.20	0.1486	2.475	42.94	0.1184
0.25	0.1506	2.342	27.90	0.07412
0.30	0.1518	2.223	19.42	0.04930
0.35	0.1523	2.116	14.36	0.03437
0.40	0.1521	2.018	10.93	0.02449
0.45	0.1512	1.930	8.506	0.01762
0.50	0.1495	1.850	6.739	0.01273
0.55	0.1472	1.775	5.406	0.00923
0.60	0.1442	1.707	4.387	0.00666
0.65	0.1404	1.644	3.587	0.00474
0.70	0.1360	1.586	2.953	0.00332
0.75	0.1309	1.533	2.431	0.00225
0.80	0.1250	1.482	2.013	0.00147
0.85	0.1184	1.436	1.667	0.00089
0.90	0.1112	1.393	1.381	0.00048
0.95	0.1032	1.354	1.134	0.00019
1.00	0.0945	1.317	0.930	0
1.10	0.0750	1.254	0.611	-0.00018
1.20	0.0527	1.208	0.443	-0.00019



In this case, it is assumed  $l_2=0.068\delta$  which is the value obtained in the experiment on the flow in the boundary region of two-dimensional free jet. Numerical values of  $\frac{\theta}{\delta}$  and  $H$  are shown by broken lines in Fig. 5 and in Table 6.

4. Momentum Equations for Turbulent Boundary Layer

From eq. (1)

$$\frac{d\theta}{dx} + \frac{\theta}{u_0} \cdot \frac{du_0}{dx}(2+H) = \zeta, \tag{14}$$

where  $\zeta = \frac{\tau_0}{\rho u_0^2}$ .

From eq. (4)

$$\frac{\varphi_1}{u_0} \cdot \frac{du_0}{dx} + \frac{\varphi_2}{\delta} \cdot \frac{d\delta}{dx} + \varphi_3 \frac{d\kappa}{dx} + \frac{\varphi_4}{\delta} = 0, \tag{15}$$

where  $\varphi_1, \varphi_2, \varphi_3$  and  $\varphi_4$  are functions of  $\kappa$  and  $\sigma$ . Replacing  $\delta$  by  $\theta$  in eq. (15) and combining with eq. (14),

$$\psi_1 \frac{d\kappa}{dx} = -\frac{\psi_2}{u_0} \cdot \frac{du_0}{dx} - \frac{\psi_3}{\theta}, \tag{16}$$

where  $\psi_1, \psi_2$  and  $\psi_3$  are functions of  $\kappa$  and  $\sigma$ .

$$\psi_1 = \frac{d(k_3 - k_1)}{d\kappa} - \frac{2k_3 - k_1 - k_5}{k_1 - k_2} \cdot \frac{d(k_1 - k_2)}{d\kappa} + k_6,$$

$$\psi_2 = k_4 + k_5 - \frac{1}{2} - \frac{1 - k_2}{k_1 - k_2} (2k_3 - k_1 - k_5),$$

$$\psi_3 = \zeta(2k_3 - k_1 - k_5) + k_7(k_1 - k_2).$$

Again replacing  $\kappa$  by  $H$ , eq. (16) becomes as follows :

$$\frac{dH}{dx} = -\frac{f_1(H)}{u_0} \cdot \frac{du_0}{dx} - \frac{f_2(H)}{\theta}. \tag{17}$$

$f_1(H)$  and  $f_2(H)$  are functions of  $H$  and  $\sigma$  and they are shown in Figs. 6 and 7 for  $\sigma=0.03, 0.04$  and  $0.05$  and in Tables 3, 4 and 5. In this calculation it is assumed that

$$\zeta = \frac{\tau_0}{\rho u_0^2} = \kappa^2 \sigma^2,$$

$\sigma^2 = \zeta_0$  being the value of  $\zeta$  for  $F(\eta)$ .

In the case of velocity distribution of eq. (10),  $\zeta = \zeta_0 =$

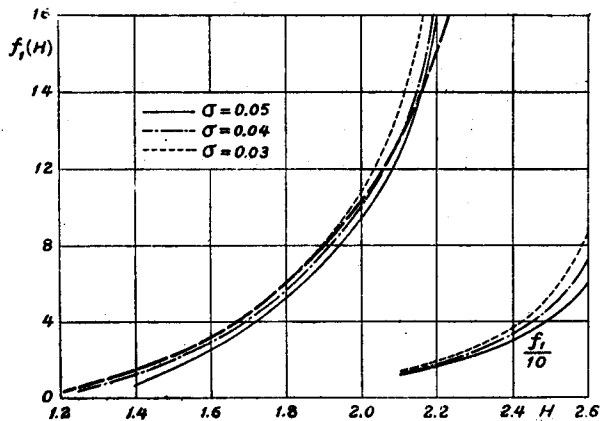


Fig. 6.

0.00212 is assumed and the calculated results are shown in Table 6 and in Figs. 6 and 7 by broken lines.\*

By solving eqs. (14) and (17), the thickness of the boundary layer and the velocity distribution in the boundary layer are determined. The velocity distribution at the separation point is given in Fig. 3 and the value of  $H$  is 2.646; hence the separation

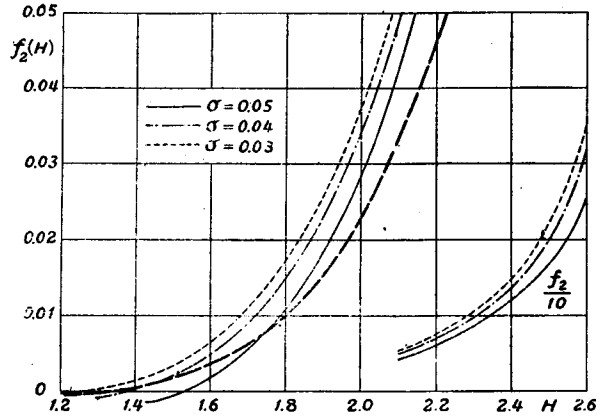


Fig. 7.

point, if it exists, is determined by  $H=2.65$ . On the other hand, in the case of accelerated flow, if  $\kappa$  reaches 1.1~1.2 according to the value of  $\sigma$ , the velocity distribution maintains the same form in such a region of flow unless  $\kappa$  diminishes with the decrease of pressure gradient.

$f_2(H)$  consists of two factors, one factor being a function of  $H$ , and the other  $\zeta$ . Let  $\zeta = \xi \left( \frac{\nu}{u_0 \theta} \right)^{\frac{1}{2}}$  and  $f_2(H) = \zeta f_3(H)$ , then from eq. (17)

$$\left( \frac{u_0 \theta}{\nu} \right)^{\frac{1}{2}} \frac{\theta}{u_0} \cdot \frac{du_0}{dx} \left( 1 - \frac{u_0}{f_1(H)} \cdot \frac{dH}{du_0} \right) = \frac{f_3(H) \xi}{f_1(H)}$$

Hence, if  $\frac{u_0}{f_1(H)} \cdot \frac{dH}{du_0}$  is a function of  $H$  alone,  $H$  is determined by Buri's parameter  $\left( \frac{u_0 \theta}{\nu} \right)^{\frac{1}{2}} \frac{\theta}{u_0} \cdot \frac{du_0}{dx}$ . But results of the experiments of both Gruschwitz and the author do not give a single relation between  $H$  and Buri's parameter.

### 5. Simplified Calculation

To calculate the boundary layer thickness and velocity distribution, it is necessary to solve simultaneous differential equations numerically. But fortunately, the momentum thickness can be calculated independently by the method originated by Buri, and this makes calculation easier than when simultaneous equations have to be solved.

In eq. (14), assume  $H=1.4$ , then

$$\frac{d\theta}{dx} + 3.4 \frac{\theta}{u_0} \cdot \frac{du_0}{dx} = \xi \left( \frac{\nu}{u_0 \theta} \right)^{\frac{1}{2}},$$

\* Gruschwitz's empirical relation can also be transformed into the same form as eq. (17). By using the velocity distribution of eq. (10) corresponding values of  $f_1(H)$  and  $f_2(H)$  are calculated. These values increase with  $H$  but their numerical values are smaller than those values given in Figs. 6 and 7.

hence

$$\left(\frac{u_0 \theta}{\nu}\right)^{\frac{1}{2}} \theta = \frac{1}{u_0^4} \left\{ \frac{5}{4} \xi \int u_0^4 dx + \text{const.} \right\}.$$

From results of several experiments, the author has obtained  $\xi=0.0136$ ; hence

$$\left(\frac{u_0 \theta}{\nu}\right)^{\frac{1}{2}} \theta = \frac{1}{u_0^4} \left\{ 0.017 \int_0^x u_0^4 dx + C \right\}, \tag{18}$$

where  $C = \left\{ u_0^4 \theta \left(\frac{u_0 \theta}{\nu}\right)^{\frac{1}{2}} \right\}_{x=0}$ .

This formula yields good results except in the neighbourhood of the separation point.

From eq. (17) for two points  $x$  and  $x + \Delta x$ , the amount of change of  $H$  in the distance of  $\Delta x$  is given by the following equation:

$$\Delta H = -f_1(H) \frac{\Delta u_0}{u_0} - f_2(H) \frac{\Delta x}{\theta}. \tag{19}$$

By using the value of  $\theta$  calculated by eq. (18) and values of  $u_0$ ,  $\Delta u_0$ ,  $f_1(H)$  and  $f_2(H)$ ,  $\Delta H$  can be calculated and  $H$  is determined.

### 6. Examples of Calculation

The above-mentioned method is applied to the experimental results of Gruschwitz. Calculation has been carried out by solving eqs. (14) and (17) by Runge-Kutta's method. Fig. 8 shows the measured velocity and calculated velocity

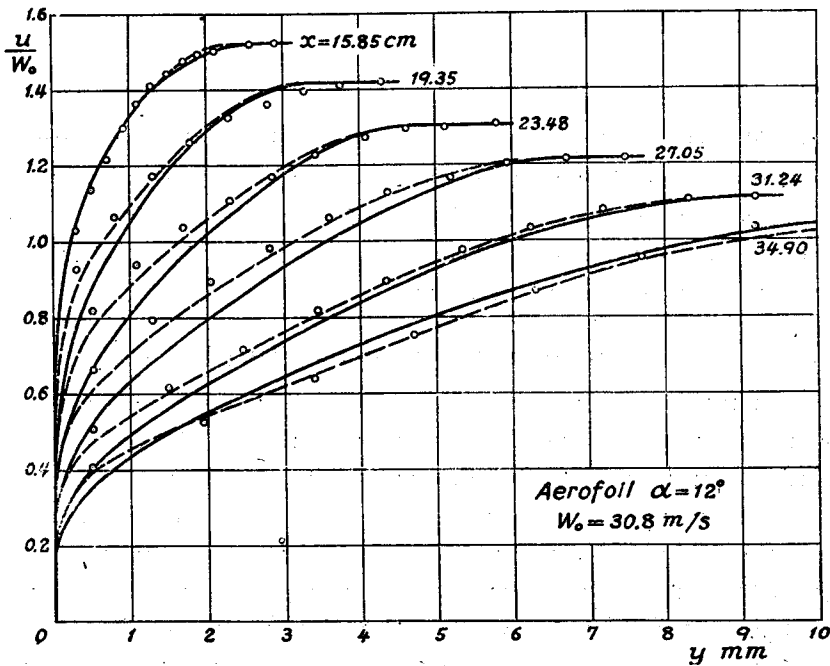


Fig. 8.

distributions in the case of aerofoil at an angle of incidence  $\alpha=12^\circ$ . The boundary layer thickness and velocity distribution in the transition region from the laminar to the turbulent flow can be roughly estimated by the present method as shown in the next paragraph. Still, there is doubt as to whether eq. (17) can be applied to such a region or not. So to compare the calculated results with the experiment in the region of turbulent flow, velocity distribution at  $x=15.85$  cm where the turbulent flow is well developed, is assumed and those on the downstream side are calculated. Points show the measured velocity and the lines are those calculated by taking  $\sigma=0.05$  and broken lines are those calculated by using the velocity distribution given by eq. (10). Fig. 9 shows the case of the test series No. 3 where

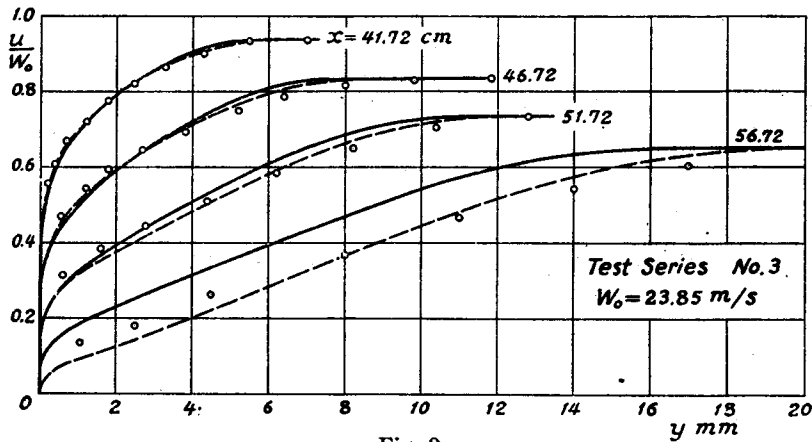


Fig. 9.

it is assumed  $\sigma=0.04$ . The calculated results coincide with experimental results fairly well but some difference is observed. Numerically it seems better to use the velocity distribution of eq. (10) and  $f_1(H)$  and  $f_2(H)$  deduced from it, though its application is limited to the case where the surface of body is smooth and Reynolds number of the boundary layer is not large.

### 7. Transition Region on the Flat Plate

In obtaining eq. (17), it is assumed that the velocity distribution is expressed with a single parameter  $\kappa$ , and that a single relation holds between velocity distribution and shearing stress distribution connected by the mixing length which is a function of  $\eta$  alone. So eq. (17) can be applied only when the velocity distribution changes gradually in the direction of flow, and it is not correct to apply this equation to the transition region from the laminar to the turbulent flow. Yet it is of some interest to estimate the length of transition region.

The case of the flow along a flat plate placed along a uniform flow is considered,

and it is assumed  $H=2.65$  at the beginning of the region. In this case eqs. (14) and (17) become as follows:

$$\frac{d\theta}{dx} = \zeta \quad \text{and} \quad \frac{dH}{dx} = -\frac{f_2(H)}{\theta}$$

$$\text{or} \quad \frac{\zeta dH}{f_2(H)} = -\frac{d\theta}{\theta}$$

These equations can easily be integrated. Fig. 10 shows the variations of  $H$ ,  $\theta$  and  $\zeta$  along the flat plate;  $x$  is the distance measured from the point where transition begins and  $\theta_0$  is the momentum thickness at the end of the laminar part.  $H$  diminishes with  $x$  and the velocity distribution approaches to the regular one asymptotically.

For example, if the length of transition region is assumed to be approximately  $150\theta_0$ ,  $\theta_0$  being 0.03 cm, then the length of transition will be 4.5 cm, and this value agrees fairly well with the experimental result of Gruschwitz.

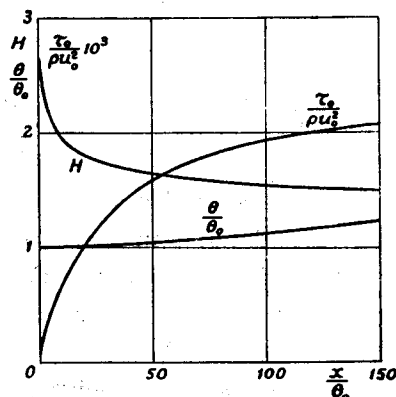


Fig. 10.

### Acknowledgement

The present investigation is a part of the author's researches supported by the Science Research Expenses of Ministry of Education and thanks are due to the Ministry of Education. The author also wishes to extend his cordial thanks to Messrs. Y. Kataoka, H. Dohata and Miss. K. Enomoto for their zealous assistance in preparing the numerical tables.

### References

- 1) Kármán, Th. v.: Ueber laminare und turbulente Reibung, Z. A. M. M. Bd. 1, 1921.
- 2) Pohlhausen, K.: Zur näherungsweise Integration der Differentialgleichung der laminaren Grenzschicht, Z. A. M. M. Bd. 1, 1921.
- 3) Buri, A.: Berechnungsgrundlage für die turbulente Grenzschicht bei beschleunigter und verzögerter Grundströmung, Dissertation Zürich, 1931.
- 4) Gruschwitz, E.: Die turbulente Reibungsschicht bei Druckabfall und Druckanstieg, Ing.-Archiv, Ed. 2, 1931.
- 5) Schultz-Grunow, F.: Neues Reibungswiderstandsgesetz für glatte Platten, Luftfahrtforschung, Bd. 17, 1940.
- 6) Nikuradse, J.: Untersuchung über die Strömungen des Wassers in konvergenten und divergenten Kanälen, Forsch.-Arb., Heft 289, 1929.
- 7) Nikuradse, J.: Turbulente Reibungsschichten an der Platte, Z. W. B.